

Study of intrinsic spin and orbital Hall effects in Pt based on a ($6s, 6p, 5d$) tight-binding model

H. KONTANI¹, M. NAITO¹, D.S. HIRASHIMA¹, K. YAMADA² and J. INOUE³

¹*Department of Physics, Nagoya University, Furo-cho, Nagoya 464-8602, Japan.*

²*College of Science and Engineering, Ritsumeikan University, Kusatsu, Shiga 525-8577, Japan.*

³*Department of Applied Physics, Nagoya University, Furo-cho, Nagoya 464-8602, Japan.*

(Dated: October 27, 2018)

We study the origin of the intrinsic spin Hall conductivity (SHC) and the d -orbital Hall conductivity (OHC) in Pt based on a multiorbital tight-binding model with spin-orbit interaction. We find that the SHC exceeds $1000 \hbar e^{-1} \cdot \Omega^{-1} \text{cm}^{-1}$ when the resistivity ρ is smaller than $\sim 10 \mu\Omega \text{cm}$, whereas it decreases to $300 \hbar e^{-1} \cdot \Omega^{-1} \text{cm}^{-1}$ when $\rho \sim 100 \mu\Omega \text{cm}$. In addition, the OHC is still larger than the SHC. The origin of the huge SHE and OHE in Pt is the large “effective magnetic flux” that is induced by the interorbital transition between d_{xy} - and $d_{x^2-y^2}$ -orbitals with the aid of the strong spin-orbit interaction.

PACS numbers:

Recently, the spin Hall effect (SHE) has attracted much attention due to its fundamental interest and its potential application in spintronics. The SHE has a close relation to the anomalous Hall effect (AHE) in ferromagnets: In 1954, Karplus and Luttinger (KL) [1] studied the Hall effect in multiband systems and found that an electric field induces a spin-dependent transverse current in the presence of spin-orbit (SO) interaction. This effect causes the AHE (transverse charge current) in ferromagnetic metals and the SHE (transverse spin current) in paramagnetic metals. These phenomena are fundamental issues in recent condensed matter physics [2–17]. In these years, great progress on the SHE in semiconductors has been made. Murakami et al. [2] and Sinova et al. [3] have studied the intrinsic (impurity-independent) SHE in semiconductors by developing the theory of KL. Now, the SHE in two-dimensional electron gas (2DEG) with a Rashba-type SO interaction is well understood [4–7]. Although the SHE in semiconductors was recognized by the optical detection of spin accumulation [8, 9], it is unfortunately too small for quantitative analysis. Therefore, materials that show a large SHE are highly desirable.

Recent experiments have revealed that the SHE also exists in metals such as Al [10] and Cl-doped ZnSe [11]. In particular, the huge spin Hall conductivity (SHC) in Pt at room temperature [$240 \hbar e^{-1} \cdot \Omega^{-1} \text{cm}^{-1}$] [13], which is 10^4 times larger than the SHC reported in semiconductors, has attracted great attention. Simple 2DEG models cannot explain this experimental fact. Recently, the present authors have studied the SHE in Sr_2RuO_4 that is described by the t_{2g} -orbital tight-binding model [14] and found that the anomalous velocity due to interorbital hopping gives rise to huge SHC in transition metals. This mechanism also causes the large AHE [15–17]. To reveal the origin of the huge SHE in Pt, we have to investigate the anomalous velocity due to the multiorbital effect by considering all the d -orbitals ($t_{2g}+e_g$ orbitals).

In this letter, we study the intrinsic SHE and the d -

orbital Hall effect (OHE) in Pt by analyzing a realistic multiorbital tight-binding model. In the low-resistivity regime where $\rho < 10 \mu\Omega \text{cm}$, both the SHC and orbital Hall conductivity (OHC) are constant of order $1000 \sim 3000 \hbar e^{-1} \cdot \Omega^{-1} \text{cm}^{-1}$, whereas they are strongly suppressed in the high-resistivity regime where $\rho \gg 10 \mu\Omega \text{cm}$. The derived coherent-incoherent crossover is a universal property of intrinsic Hall effects [15, 17]. Both the SHE and OHE originate from a kind of Peierls phase factor due to the “effective magnetic flux” [14] that is induced by a combination of the angular dependence of d -orbital wave functions and SO interaction. In Pt, the dominant contribution to the SHE is given by the d_{xy} -orbital (in t_{2g}) and the $d_{x^2-y^2}$ -orbital (in e_g). Therefore, both the t_{2g} - and e_g -orbitals should be taken into account to explain the huge SHE in Pt.

Pt has a face-centered cubic (FCC) structure with $a = 3.9 \text{ \AA}$, and the nearest inter-atomic distance is 2.8 \AA . In the present study, we use the Naval Research Laboratory tight-binding (NRL-TB) model [18, 19] to describe the bandstructure in Pt. The NRL-TB model employs the scheme of the two-center, non-orthogonal Slater-Koster (SK) Hamiltonian [20]. The SK parameters are represented with distance- and environment-dependent parameters that are determined so that the obtained total energy and the band structures agree well with those obtained by the first-principles calculations. Here, we take into account $6s$, $6p$, and $5d$ orbitals (in total, nine) and hopping integrals up to the sixth nearest neighbor sites. The electron number per Pt atom is ten. The NRL-TB model uses non-orthogonal bases, but we neglect the overlap integrals between different sites in this study for simplicity [21]. This simplification significantly changes the dispersion of the s -band far from the Fermi level, while that of the band structure near the Fermi energy is little affected. In the presence of the SO interaction for $5d$ electrons $H_{\text{SO}} = \lambda \sum_i (\mathbf{l} \cdot \mathbf{s})_i$, the total

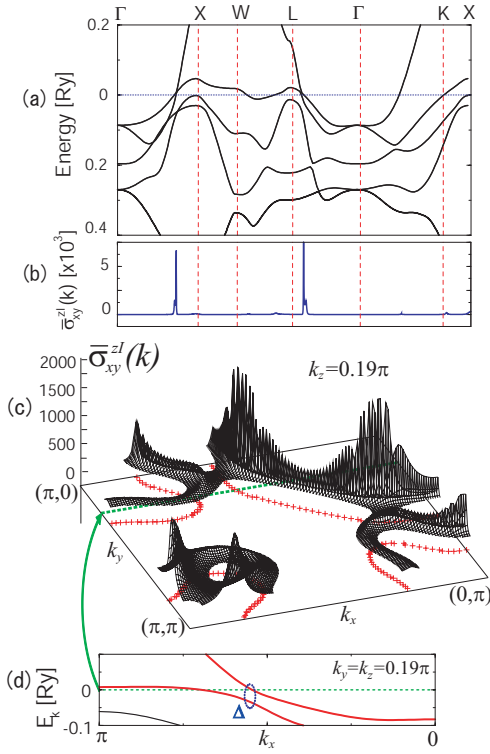


FIG. 1: (Color online) (a) Band structure of a $(6s, 6p, 5d)$ tight-binding model for Pt ($\lambda = 0.04$). $\Gamma = (0, 0, 0)$, $X = (\pi, 0, 0)$, $W = (\pi, \pi/2, 0)$, $L = (\pi/2, \pi/2, \pi/2)$, and $K = (3\pi/4, 3\pi/4, 0)$. (b) $\bar{\sigma}_{xy}^z(\mathbf{k})$ for $\gamma = 0.002$ along Γ -X. (c) $\bar{\sigma}_{xy}^z(\mathbf{k})$ on the plane $k_z = 0.19\pi$, which is plotted only for $\bar{\sigma}_{xy}^z(\mathbf{k}) > 25$. The crosses represent the Fermi surfaces. (d) k_x -dependence of E^l for $k_y = k_z = 0.19\pi$; the minimum bandsplitting near the Fermi level Δ is ~ 0.035 .

Hamiltonian becomes

$$\hat{H} = \begin{pmatrix} \hat{H}_0 + \lambda \hat{l}_z/2 & \lambda(\hat{l}_x - i\hat{l}_y)/2 \\ \lambda(\hat{l}_x + i\hat{l}_y)/2 & \hat{H}_0 - \lambda \hat{l}_z/2 \end{pmatrix}, \quad (1)$$

where \hat{H}_0 is a 9×9 matrix given by the NRL-TB model. The matrix elements of \mathbf{l} are given in ref. [22]. The bandstructure obtained for the $(6s, 6p, 5d)$ tight-binding model with $\lambda = 0.04$ Ry is shown in Fig. 1 (a), which is in good agreement with the result of a relativistic first-principles calculation [23, 24] near the Fermi level. According to optical spectroscopy, $\lambda = 0.03$ Ry for a $5d$ electron in Pt, and $\lambda = 0.013$ Ry for a $4d$ electron in Pd [22]. Hereafter, we set the unit of energy Ry; 1 Ry = 13.6 eV. Based on the NRL-TB model, spin wave excitations and the electron self-energy corrections in the ferromagnetic Fe are studied using the random-phase approximation [25].

The 18×18 matrix form of the retarded Green function is given by $\hat{G}^R(\mathbf{k}, \omega) = (\omega + \mu - \hat{H} + i\Gamma)^{-1}$, where μ is the chemical potential and Γ is the imaginary part of the \mathbf{k} -independent self-energy (damping rate) due to scattering

by local impurities (or inelastic scattering by phonons).

The charge current in the present model is

$$\hat{J}_\mu^C = \begin{pmatrix} \hat{J}_\mu^C & 0 \\ 0 & \hat{J}_\mu^C \end{pmatrix}. \quad (2)$$

Here, $\hat{J}_\mu^C = -e \frac{\partial \hat{H}_0}{\partial k_\mu}$, where $-e$ is the electron charge and $\mu = x, y$. In this case, the atomic SO interaction is not involved in the charge current since it is \mathbf{k} -independent. Then, the s_z -spin current $\hat{J}_\mu^S = \{\hat{J}_\mu^C, \hat{s}_z\}/2$ is expressed as

$$\hat{J}_\mu^S = (-\hbar/e) \begin{pmatrix} \hat{J}_\mu^C & 0 \\ 0 & -\hat{J}_\mu^C \end{pmatrix}. \quad (3)$$

Here, we discuss the current vertex correction (CVC) due to the local impurity potentials in the Born approximation, which is given by $\Delta \hat{J}_\mu^C \propto \sum_{\mathbf{k}} \hat{G}^A \hat{J}_\mu^C \hat{G}^R$. When α is one of the p -orbitals and β is one of the (s, d) -orbitals, $(\hat{H}_0(\mathbf{k}))_{\alpha, \beta}$ is an odd function with respect to $\mathbf{k} \leftrightarrow -\mathbf{k}$, and therefore the (α, β) -component of $(\partial/\partial k_\mu) \hat{G} = \hat{G} \hat{J}_\mu^C \hat{G}$ is an even function. Note that $|p_\nu\rangle \rightarrow -|p_\nu\rangle$ ($\nu = x, y, z$) under the parity transformation. Thus, $(\Delta \hat{J}_\mu^C)_{\alpha, \beta}$ is finite only when either α or β is a p -orbital. In Pt, however, we have verified that the CVC affects the SHE only slightly [less than 5%] since the $6p$ -level is 20 eV higher than the Fermi level μ and the p -electron density of states (DOS) at μ is very small. For this reason, we disregard the CVC hereafter.

According to the linear response theory [26], the SHC is given by $\sigma_{xy}^z = \sigma_{xy}^{zI} + \sigma_{xy}^{zII}$, where

$$\begin{aligned} \sigma_{xy}^{zI} &= \frac{1}{2\pi N} \sum_{\mathbf{k}} \text{Tr} \left[\hat{j}_x^S \hat{G}^R \hat{j}_y^C \hat{G}^A \right]_{\omega=0}, \quad (4) \\ \sigma_{xy}^{zII} &= \frac{-1}{4\pi N} \sum_{\mathbf{k}} \int_{-\infty}^0 d\omega \text{Tr} \left[\hat{j}_x^S \frac{\partial \hat{G}^R}{\partial \omega} \hat{j}_y^C \hat{G}^R \right. \\ &\quad \left. - \hat{j}_x^S \hat{G}^R \hat{j}_y^C \frac{\partial \hat{G}^R}{\partial \omega} - \langle R \rightarrow A \rangle \right]. \quad (5) \end{aligned}$$

Here, I and II represent the ‘‘Fermi surface term’’ and the ‘‘Fermi sea term’’, respectively. In the same way, the OHC of the Fermi surface term O_{xy}^{zI} and that of the Fermi sea term O_{xy}^{zII} are given by eqs. (4) and (5), respectively, by replacing \hat{j}_x^S with the l_z -orbital current $\hat{J}_x^O = \{\hat{J}_x^C, \hat{l}_z\}/2$. Because of the cubic symmetry of Pt, $\sigma_{\mu\nu}^\delta = \sigma_{xy}^z \cdot \epsilon_{\mu\nu\delta}$ and $O_{\mu\nu}^\delta = O_{xy}^z \cdot \epsilon_{\mu\nu\delta}$, where $\mu, \nu, \delta = x, y, z$ and $\epsilon_{\mu\nu\delta}$ is the antisymmetrized tensor with $\epsilon_{xyz} = 1$.

When $\Gamma_{\alpha\beta} = \gamma \delta_{\alpha\beta}$ (constant γ approximation), ω -integration in eq. (5) can be performed analytically as

shown in ref. [15]: Then, $\sigma_{xy}^{zII} = \sigma_{xy}^{zIIa} + \sigma_{xy}^{zIIb}$, where

$$\sigma_{xy}^{zIIa} = \frac{-1}{2\pi N} \sum_{\mathbf{k}, l \neq m} \text{Im} \left\{ (J_x^S)^{ml} (J_y^C)^{lm} \right\} \frac{1}{E_{\mathbf{k}}^l - E_{\mathbf{k}}^m} \times \text{Im} \left\{ \frac{E_{\mathbf{k}}^l + E_{\mathbf{k}}^m - 2i\gamma}{(E_{\mathbf{k}}^l - i\gamma)(E_{\mathbf{k}}^m - i\gamma)} \right\}, \quad (6)$$

$$\sigma_{xy}^{zIIb} = \frac{1}{\pi N} \sum_{\mathbf{k}, l \neq m} \text{Im} \left\{ (J_x^S)^{ml} (J_y^C)^{lm} \right\} \frac{1}{(E_{\mathbf{k}}^l - E_{\mathbf{k}}^m)^2} \times \text{Im} \left\{ \ln \left(\frac{E_{\mathbf{k}}^l - i\gamma}{E_{\mathbf{k}}^m - i\gamma} \right) \right\}, \quad (7)$$

where l, m represent the band indices. $E_{\mathbf{k}}^l$ is the l th eigenenergy of \hat{H} measured from the chemical potential μ ; $\sum_{\alpha, \beta} U_{l\alpha}^\dagger H_0^{\alpha\beta} U_{\beta m} = E_{\mathbf{k}}^l \delta_{lm}$, where α, β are the orbital indices and U is a \mathbf{k} -dependent unitary matrix. $(J_x^S)^{ml}$ in eqs. (6) and (7) is given by $\sum_{\alpha, \beta} U_{l\alpha}^\dagger (J_x^S)^{\alpha\beta} U_{\beta m}$.

In the Born approximation, $\hat{\Gamma}$ in the Green function is given by $n_{\text{imp}} I^2 \frac{1}{N} \sum_{\mathbf{k}} \text{Im}(\hat{G}^A(0) - \hat{G}^R(0))$, where I is the local impurity potential and n_{imp} is the impurity density. When $\lambda/E_F \ll 1$, $\hat{\Gamma}$ is almost diagonal with respect to the orbital index; $\Gamma_{\alpha, \beta} = \gamma_{\alpha} \delta_{\alpha, \beta}$ [14]. In the case of Sr_2RuO_4 , the SHC in the Born approximation is nearly three times greater than that in the constant γ approximation [14]. In Pt, in contrast, we have verified that both approximations give a similar SHC in the clean limit. For this reason, we use the constant γ approximation hereafter.

Here, we determine the part of the Fermi surface from which the SHC originates: In Fig. 1 (b) and (c), we show $\bar{\sigma}_{xy}^{zI}(\mathbf{k}) \equiv \frac{1}{8} \sum_{k'_x = \pm k_x} \sum_{k'_y = \pm k_y} \sum_{k'_z = \pm k_z} \sigma_{xy}^{zI}(\mathbf{k}')$, where $\sigma_{xy}^{zI}(\mathbf{k})$ is the integrand in eq. (4). [Apparently, $\frac{1}{N} \sum_{\mathbf{k}} \bar{\sigma}_{xy}^{zI}(\mathbf{k}) = \sigma_{xy}^{zI}$.] $\bar{\sigma}_{xy}^z(\mathbf{k})$ is finite only on the Fermi surface, and it takes huge values at $(0.73\pi, 0, 0)$ (on Γ -X) and at $(0.42\pi, 0.42\pi, 0.42\pi)$ (on L- Γ) since two bands are very close on the Fermi level in the present model. However, the contribution of these two points to the SHC is small after taking the \mathbf{k} -summation. The dominant contribution comes from a wide area around $(0.19\pi, 0.19\pi, 0.57\pi)$ as shown in Fig. 1 (d). Here, the bandsplitting Δ near the Fermi level is 0.035.

Now, we perform the numerical calculation of the SHC, using $128^3 \sim 512^3$ \mathbf{k} -meshes. Figure 2 (a) shows the λ -dependence of the total SHC $\sigma_{xy}^z = \sigma_{xy}^{zI} + \sigma_{xy}^{zII}$ for $\gamma = 0.02$, which is smaller than $\Delta = 0.035$. σ_{xy}^{zII} represents the Fermi sea term in eq. (5). Apparently, $\sigma_{xy}^z \approx \sigma_{xy}^{zI} \gg \sigma_{xy}^{zII}$ is realized. σ_{xy}^z increases with λ monotonically, and it reaches $1000 \hbar e^{-1} \cdot \Omega^{-1} \text{cm}^{-1}$ at $\lambda = 0.03$. To clarify the origin of the SHE, we study the SHC when the SO interaction is anisotropic: As shown in Fig. 2 (a), σ_{xy}^z for $H_{\text{SO}} = \lambda \sum_i (l_x s_x + l_y s_y)_i$ is much smaller than that in the isotropic case where $H_{\text{SO}} = \lambda \sum_i (l \cdot \mathbf{s})_i$. On the other hand, σ_{xy}^z for $H_{\text{SO}} = \lambda \sum_i (l_z s_z)_i$ almost coincides with that in the isotropic case. Therefore, it

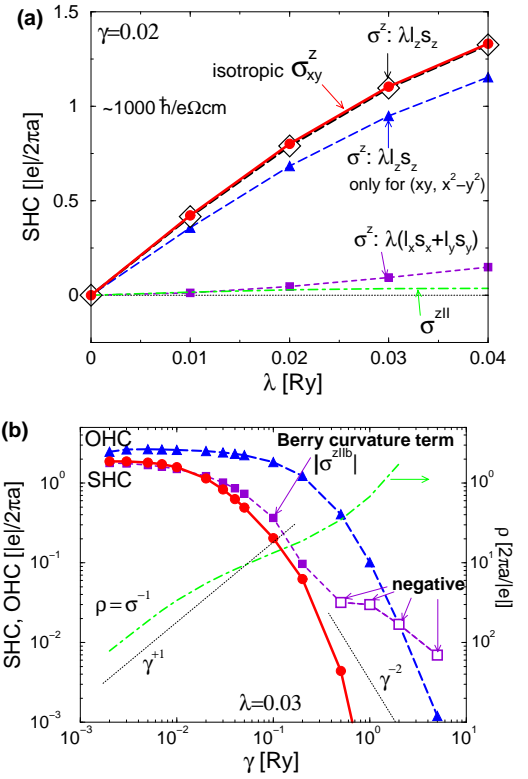


FIG. 2: (Color online) (a) λ -dependence of the SHC. The relation $\sigma_{xy}^z \approx \sigma_{xy}^{zI} \gg \sigma_{xy}^{zII}$ is realized. The matrix element of the SO interaction between the d_{xy} -orbital and the $d_{x^2-y^2}$ -orbital gives the dominant contribution to the SHC. Note that $1 [e/2\pi a] \approx 1000 \hbar e^{-1} \cdot \Omega^{-1} \text{cm}^{-1}$ for $a = 4 \text{ \AA}$. (b) Crossover behaviors of the SHC and OHC at $\gamma \sim \Delta \approx 0.035$. ρ is approximately proportional to γ . $\rho = 1$ corresponds to $1000 \mu\Omega \text{cm}$.

is concluded that the z -component of the SO interaction gives the decisive contribution to the SHC. The matrix element of l_z is finite only for $\langle yz|l_z|zx \rangle = -\langle zx|l_z|yz \rangle = i$ and $\langle xy|l_z|x^2-y^2 \rangle = -\langle x^2-y^2|l_z|xy \rangle = 2i$. Among them, the d_{xy} - and $d_{x^2-y^2}$ -orbitals, both of which are given by the linear combinations of $l_z = \pm 2$, cause a dominant contribution to the SHC as shown in Fig. 2 (a).

Here, we discuss the γ -dependence of the SHC and OHC: When γ is sufficiently small, these intrinsic Hall conductivities are proportional to the lifetime of the interband particle-hole excitation: \hbar/Δ [1–3, 14, 15, 17]. In fact, Fig. 2 (b) shows that both the SHC and OHC for $\lambda = 0.03$ [22] are independent of γ for $\gamma \ll \Delta \sim 0.035$. In the high-resistivity regime where $\gamma \gg \Delta$, both SHC and OHC decrease drastically with γ since the interband excitation is suppressed when the quasiparticle lifetime \hbar/γ is shorter than \hbar/Δ . This coherent-incoherent crossover of the intrinsic Hall conductivities ($\sigma_{xy} = \text{const.}$ for $\gamma \ll \Delta$ and $\sigma_{xy} \propto \rho^{-2}$ for $\gamma \gg \Delta$) has been analyzed theoretically in refs. [15, 17]. In Pt, the SHC decreases

much faster than ρ^{-2} in the high-resistivity regime and the SHC becomes negative for $\gamma > 1$, which may be due to a complex multiband structure. If we put $\gamma \sim 0.07$, $\rho \sim 0.1 [|e|/2\pi a] \sim 100 \mu\Omega\text{cm}$. Then, the obtained SHC is $\sim 300 \hbar e^{-1} \cdot \Omega^{-1}\text{cm}^{-1}$, which is close to the experimental SHC of Pt [13]. In the experimental situation, γ in Fig. 2 (b) corresponds to $\hbar/2\tau$ within the spin diffusion length in Pt (~ 10 nm) from the interface of the junction, which might be larger than the bulk value of γ .

We comment on σ_{xy}^{zIIb} , which is frequently called the ‘‘Berry curvature term’’. When $\Gamma_{\alpha\beta} = \gamma\delta_{\alpha\beta}$ and $\gamma \rightarrow 0$, $\sigma_{xy}^z = \sigma_{xy}^{zIIb} \approx \sigma_{xy}^{zI}$ [15]. However, σ_{xy}^{zIIb} is totally different from σ_{xy}^z in the high-resistivity regime as shown in Fig. 2 (b), since the cancellation between σ_{xy}^{zI} and σ_{xy}^{zIIa} becomes worse when γ is large. In many systems including Pt, $\sigma_{xy}^z \approx \sigma_{xy}^{zI}$ is realized for a wide range of parameters [15].

We briefly discuss the SHC using the Born approximation, where γ_α is proportional to the DOS for the α -orbital, $\rho_\alpha(0)$. When γ_α is α -dependent, $\sigma_{xy}^{zIIb} \neq \sigma_{xy}^z$ even in the clean limit [14]. In fact, the SHC in Sr_2RuO_4 given by the Born approximation is much larger than that given by the constant γ approximation since the α -dependence of $\rho_\alpha(0)$ is large [14]. In Pt, however, both approximations give similar results. For this reason, we use the constant γ approximation.

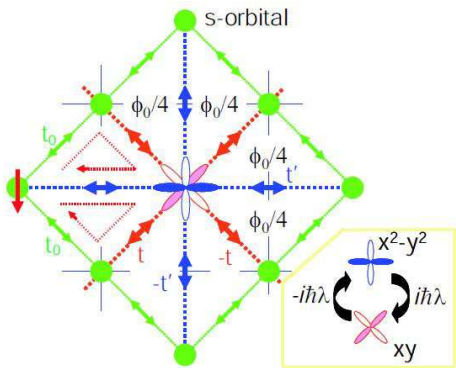


FIG. 3: (Color online) Effective magnetic flux for \uparrow -electron in the two-dimensional Pt model. This is the origin of the huge SHC and AHC in Pt.

Figure 3 shows the FCC crystal structure of Pt on the xy -plane. Based on this two-dimensional model, we explain an intuitive reason why the huge SHC appears in Pt, by considering only d_{xy} -, $d_{x^2-y^2}$ -, and s -orbitals. $\pm t$ represents the hopping integrals between the nearest neighbor d_{xy} -orbital and s -orbital, and $\pm t'$ is used for the next nearest neighbor $d_{x^2-y^2}$ -orbital and s -orbital. Both the hopping integrals change their signs by rotation by $\pi/2$. Here, we consider the motion of a \uparrow -spin electron on the left side of Fig. 3 along a triangle of a half unit cell: An electron in the d_{xy} -orbital can transfer to the $d_{x^2-y^2}$ -orbital and vice versa using the SO interaction for a \uparrow -electron $\hbar\lambda\hat{l}_z/2$; $\langle xy|\hat{l}_z|x^2-y^2\rangle = -\langle x^2-y^2|\hat{l}_z|xy\rangle = 2i$.

By considering the sign of the interorbital hopping integral ($\pm t$ and $\pm t'$) and matrix elements of the SO interaction, we can verify that a clockwise (anticlockwise) motion along any triangle path with the SO interaction causes the factor $+i$ ($-i$). This factor can be interpreted as the Aharonov-Bohm phase factor $e^{2\pi i\phi/\phi_0}$ [$\phi_0 = \hbar c/|e|$], where ϕ represents the ‘‘effective magnetic flux’’ [14] $\phi = \oint \mathbf{A}d\mathbf{r} = \pm\phi_0/4$. This effective magnetic flux gives rise to the SHC of order $O(\lambda)$.

We also discuss the origin of the OHE by considering the motion of an electron with $|l_z = +2\rangle \propto |x^2-y^2\rangle + i|xy\rangle$. We can show that an electron with $|l_z = \pm 2\rangle$ in Pt acquires the Aharonov-Bohm phase, which gives rise to the OHC of order $O(\lambda^0)$ [14].

In summary, we have studied the origin of huge SHC and OHC in Pt using a (6s, 6p, 5d) tight-binding model, and found that the SHC reaches $1000 \hbar e^{-1} \cdot \Omega^{-1}\text{cm}^{-1}$ in the low-resistivity regime where $\rho < 10 \mu\Omega\text{cm}$. Other significant findings of the present study are that (i) the OHC is still larger than the SHC in Pt, which will cause large surface magnetization of Pt; (ii) the huge SHC and OHC originate from the effective magnetic flux created by the d_{xy} - and $d_{x^2-y^2}$ -orbitals; and (iii) the coherent-incoherent crossover behaviors of the SHC and OHC are derived by taking both the I -term and II -term into account correctly. When $\rho \sim 100 \mu\Omega\text{cm}$, the obtained SHC becomes comparable with the experimental value $240 \hbar e^{-1} \cdot \Omega^{-1}\text{cm}^{-1}$. Note that ρ in the present calculation corresponds to the resistivity within the spin diffusion length (~ 10 nm) from the interface of the junction. We comment that the effect of the overlap integral reduces the magnitude of the SHC for Pt to some extent [21]. Finally, we discuss the role of the Coulomb interaction: Although the SHC is independent of the renormalization factor $z = (1 - \partial\Sigma(\omega)/\partial\omega)^{-1}|_{\omega=0}$ ($= m/m^*$) [14, 15], it will depend on the ω -dependence of $\gamma(\omega)$ as well as the CVC due to the Coulomb interaction. They are important future issues.

During the preparation of this paper, we found a paper where the SHC was calculated based on a relativistic first-principles calculation [27]. Only the Berry curvature term given by eq. (7) was calculated, which is not justified in the high-resistivity regime ($\gamma \gg \Delta$) [15].

The authors acknowledge fruitful discussions with Y. Otani, T. Kimura, M. Sato, and T. Tanaka. This work was supported by the Next Generation supercomputing Project, Nanoscience Program, Grant-in-Aid for the 21st Century COE ‘‘Frontiers of Computational Science’’, and Grant-in-Aid for Scientific Research from the Ministry of Education, Science, Sports and Culture of Japan.

[1] R. Karplus and J. M. Luttinger: Phys. Rev. **95** (1954) 1154.

- [2] S. Murakami, N. Nagaosa and S.C. Zhang: Phys. Rev. B **69** (2004) 235206.
- [3] J. Sinova, D. Culcer, Q. Niu, N. A. Sinitsyn, T. Jungwirth, and A. H. MacDonald: Phys. Rev. Lett. **92** (2004) 126603.
- [4] J. Inoue et al., G. E. W. Bauer, and L. W. Molenkamp: Phys. Rev. **B70** (2004) 041303(R).
- [5] R. Raimondi and P. Schwab, Phys. Rev. B **71** (2005) 033311.
- [6] E. I. Rashba, Phys. Rev. B **70** (2004) 201309(R).
- [7] J. Inoue, T. Kato, Y. Ishikawa, H. Itoh, G. E. W. Bauer, and L. W. Molenkamp: Phys. Rev. Lett., **97** (2006) 46604.
- [8] Y. K. Kato, R.C. Myers, A.C. Gossard, and D.D. Awschalom: Science **306** (2004) 1910; V. Sih, R. C. Myers, Y. K. Kato, W. H. Lau, A. C. Gossard and D. D. Awschalom: Nature Physics **1** (2005) 31.
- [9] J. Wunderlich, B. Kaestner, J. Sinova, and T. Jungwirth: Phys. Rev. Lett. **94** (2005) 047204.
- [10] S. O. Valenzuela and M. Tinkham: Nature **442** (2006) 176.
- [11] N.P. Stern, S. Ghosh, G. Xiang, M. Zhu, N. Samarth, and D. D. Awschalom: Phys. Rev. Lett. **97** (2006) 126603.
- [12] E. Saitoh, M. Ueda, H. Miyajima and G. Tatara, Appl. Phys. Lett. **88** (2006) 182509.
- [13] T. Kimura, Y. Otani, T. Sato, S. Takahashi, and S. Maekawa: Phys. Rev. Lett. **98** (2007) 156601.
- [14] H. Kontani, T. Tanaka, D.S. Hirashima, K. Yamada, and J. Inoue: cond-mat/0702447.
- [15] H. Kontani, T. Tanaka, and K. Yamada: Phys. Rev. B **75** (2007) 184416.
- [16] M. Miyazawa, H. Kontani, and K. Yamada: J. Phys. Soc. Jpn. **68** (1999) 1625.
- [17] H. Kontani and K. Yamada, J. Phys. Soc. Jpn. **63** (1994) 2627.
- [18] M.J. Mehl and D.A. Papaconstantopoulos: Phys. Rev. B **54** (1996) 4519.
- [19] D. A. Papaconstantopoulos and M.J. Mehl: J. Phys.: Condens. Matter **15** (2003) R413.
- [20] J.C. Slater and G.F. Koster: Phys. Rev. **94** (1954) 1498.
- [21] T. Tanaka et al., arXiv:0711.1263; in the presence of overlap integrals between different sites, the current is $\hat{J}_\mu^C = -e \frac{\partial \hat{H}_0}{\partial k_\mu} - e \{ \hat{H}_0, \frac{\partial \hat{O}^{-1}}{\partial k_\mu} \hat{O} \} / 2$, where \hat{O} is the overlap integral matrix. We verified that the second term does not change the overall behavior of the SHC for Pt, although it reduces the magnitude of the SHC by approximately 50%.
- [22] J. Friedel, P. Lengart and G. Leman: J. Phys. Chem. Solids, **25** (1964) 781.
- [23] O.K. Andersen, Phys. Rev. B **2** (1970) 883.
- [24] S. B. der Kellen and A. J. Freeman: Phys. Rev. B **54** (1996) 11187.
- [25] M. Naito and D.S. Hirashima: J. Phys. Soc. Jpn. **76** 044703 (2007).
- [26] P. Streda: J. Phys. C: Solid State Phys. **15** (1982) L717.
- [27] G.Y. Guo, S. Murakami, T.-W. Chen, N. Nagaosa, cond-mat/0705.0409.